Available online at www.sciencedirect.com
SCIENCE DIRECT®
Bioorganic & Medicinal Chemistry 13 (2005) 735–743
Bioorganic & Medicinal Chemistry

Synthesis and in vivo biodistribution of BPA–Gd–DTPA complex as a potential MRI contrast carrier for neutron capture therapy

Kazunori Takahashi,[a] Hiroyuki Nakamura,[b] Shozo Furumoto,[c] Kazuyoshi Yamamoto,[d] Hiroshi Fukuda,[c,*] Akira Matsumura[e] and Yoshinori Yamamoto[a,*]

[a]*Department of Chemistry, Graduate School of Science, Tohoku University, Sendai 980-8578, Japan*
[b]*Department of Chemistry, Faculty of Science, Gakushuin University, Tokyo 171-8588, Japan*
[c]*Institute of Development, Aging and Cancer, Tohoku University, Sendai 980-8575, Japan*
[d]*Japan Atomic Energy Research Institute at Tokai, Ibaragi 319-1195, Japan*
[e]*Department of Neurosurgery, Institute of Clinical Medicine, University of Tsukuba, Ibaraki 305-8575, Japan*

Received 27 September 2004; revised 21 October 2004; accepted 21 October 2004
Available online 21 November 2004

Abstract—*p*-Boronophenylalanine (BPA) conjugated Gd–DTPA complex (**3**) was synthesized from the active methyne compound **6**, the allylic carbonate **7**, and BPA by the palladium-catalyzed allylation reaction followed by the DCC coupling reaction. The in vivo biodistribution of complex **3** was evaluated by prompt gamma-ray analysis and α-autoradiography using the tumor-bearing rats. High accumulation of gadolinium was observed in the kidney and the %ID values were 0.17 and 0.088 at 20 and 60 min after injection of **3**, respectively. The accumulation was also observed in the tumor and the %ID values were 0.010 and 0.0025 at 20 and 60 min after injection, respectively. The visualization experiment of boron distribution in the tumor-bearing rat by α-autoradiography indicates that boron was accumulated in the tumor and the intestines at 20 min after injection.

1. Introduction

Neutron capture therapy (NCT), as one of the radiotherapies of cancers, has gained intense interest in recent years.[1–4] This therapy is a binary system, which involves the use of two components: thermal neutrons and nuclides possessing high thermal neutron capture cross section. Although each component should be relatively innocuous to mammalian cells, their combination generates a highly lethal cytocidal effect. Among various nuclides that possess usual capacity for absorbing thermal neutrons, boron-10 and gadolinium-157 have been focused on NCT as a nonradioactive nuclide. So far, *p*-boronophenylalanine (BPA)[5–7] and mercaptoundecahydrododecaborate (BSH)[8–11] have been utilized for NCT and it is required to monitor the boron concentrations in the tumor and the surrounding tissues before irradiation of neutron in order to improve and optimize efficient NCT treatment. Positron emission tomography (PET) using fluorine-18-labeled fluoroboronophenylalanine (^{18}F-BPA) has been developed for this purpose and ^{18}F-BPA is now utilized not only for the estimation of the boron distribution but also for the prognostic indicator in patients with gliomas.[12] As an alternative monitoring method of the distribution of a carrier, magnetic resonance imaging (MRI) of boron-11 has been examined.[13–16] However, the actual nucleus for neutron capture reaction is boron-10, therefore, the administration of extra amounts of boron-11 compound, which does not undergo the nucleic reaction on NCT, is needed for MR imaging. Kahl and co-workers have succeeded in the synthesis of Mn-boronated porphyrin (BOPP) complex and visualizing the distribution of Mn by MRI.[17,18]

Gd–DTPA (Magnevist®) (**1**) is known as a MRI contrast agent and has been utilized for the diagnosis of patients with gliomas because this complex is able to

Keywords: MRI; Neutron capture therapy; *p*-Boronophenylalanine; Gadolinium complex; Gd–DTPA complex; Biodistribution.
* Corresponding authors. Tel.: +81 222176581; fax: +81 222176784; e-mail: tl@yamamoto1.chem.tohoku.ac.jp

0968-0896/$ - see front matter © 2004 Elsevier Ltd. All rights reserved.
doi:10.1016/j.bmc.2004.10.046

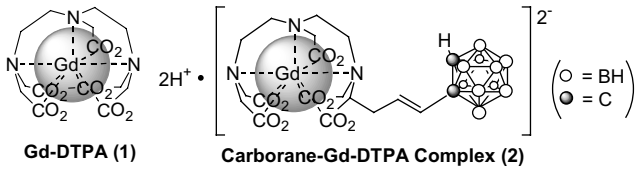

Figure 1.

pass through the disrupted blood–brain barrier and enter into the tumor tissue (Fig. 1).[19–24] Gadolinium is paramagnetic, and its effect on the contrast of the images can be best seen on T_1-weighted images with short repetition times. Furthermore, the thermal neutron capture cross section of gadolinium-157 is the largest (255,000 b) among all the stable isotopes, and it is about 66 times as large as that of boron-10 (3838 b). Matsumura and co-workers examined the visualization of Mn–metalloporphyrin–Gd–DTPA in rats using MRI for the possibility of Gd-NCT.[25–27]

We recently developed a method for the preparation of DTPA-bifunctional chelating agents in which a second functional group is attached to DTPA carbon framework through C–C bond.[28–31] This method enables us to introduce a second functional group into DTPA framework without losing one of the five carboxyl groups, whereas a general method for coupling DTPA with the second functional group is based on the conversion of one of five carboxyl groups of DTPA into an ester or an amide to produce the corresponding tetraacid derivatives.[32] Reduction of the number of carboxylic acids that are capable of coordinating to a metal ion, may cause the liberation of a metal ion in vivo.[32,33] We previously reported the synthesis of the carborane conjugated Gd–DTPA complex (**2**)[28] through C–C bond and succeeded in the visualization of the biodistribution of complex **2** in rats by MRI (Fig. 1). The visualization experiments using α-autoradiography also indicated that complex **2** was accumulated into the necrosis part of a tumor tissue.[29,30] We therefore focused on BPA as an alternative second functional group of a Gd–DTPA complex for a potential MRI contrast carrier. In this paper, we report the synthesis of *p*-boronophenylalanine (BPA) conjugated Gd–DTPA complex (**3**) and its biodistribution in the tumor-bearing rats.

2. Result and discussion

2.1. Chemistry

2.1.1. Design of BPA-conjugated Gd–DTPA complex (3). Our molecular design of BPA-conjugated Gd–DTPA complex is shown in Scheme 1. The molecule consists of three parts; a Gd–DTPA complex as an MR imaging moiety, a BPA as a biofunctional group, and a linker, and these three moieties can be connected by the palladium-catalyzed Tsuji–Trost type allylation and the amide bond formation. Therefore, we decided to synthesize the precursors **4** from the hexaethyl ester **6**[28] and the

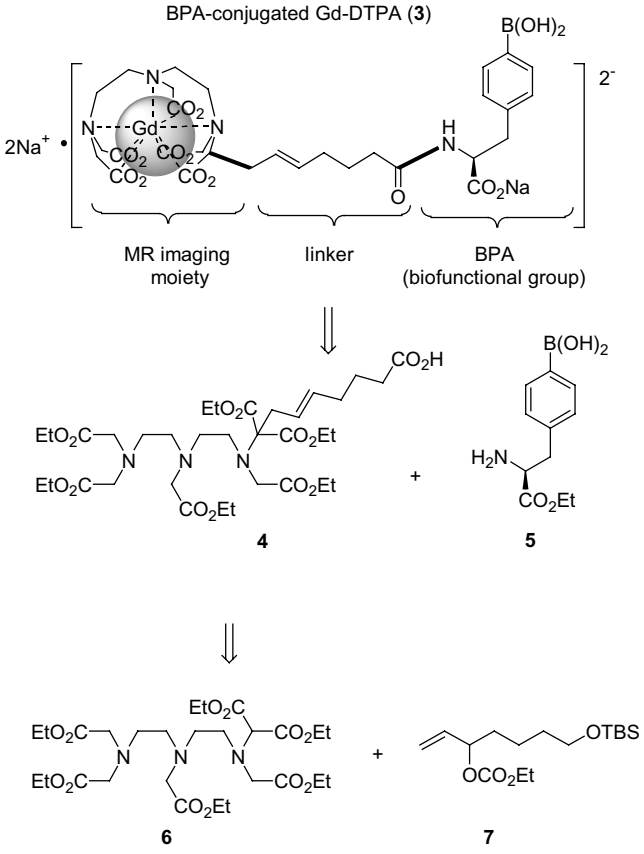

Scheme 1. Design of BPA-conjugated Gd–DTPA complex **3**.

allylic carbonate **7**, since this strategy can be utilized for introduction of various amines and amino acids as a biofunctional group into the Gd–DTPA complex by the amide bond formation.

2.1.2. Synthesis of the allylic carbonate 7. We first synthesized the allylic carbonate **7**, as a linker, from commercially available 1,5-pentanediol as shown in Scheme 2. Selective protection of 1,5-pentanediol with TBSCl was carried out in DMF at 0 °C to give the corresponding monosilylated alcohol **8** in 74% yield. The alcohol **8** was oxidized with 2,2,6,6-tetramethyl-1-piperidinyloxide (TEMPO) to give the aldehyde **9** in 92% yield. The addition of vinyl magnesium bromide to **9**, followed by the treatment with ethyl chloroformate gave the allylic carbonate **7** in 78% yield.

2.1.3. Synthesis of the precursor 4. The synthesis of the precursor **4** of the BPA–DTPA conjugate is shown in Scheme 3. The DTPA hexaethyl ester **6**, which has an active methyne moiety in a molecule, was treated with **7** under the Tsuji–Trost conditions[34] to give the allylation product **10** in 83% yield. Desilylation of **10** with TBAF afforded the alcohol **11** in 90% yield. Oxidation of **11** using SO_3·pyridine complex gave the aldehyde **12** in an essentially quantitative yield. It should be noted that Swern oxidation and TEMPO oxidation were not effective for the synthesis of **12**. Further oxidation was carried out with $NaClO_2$ to give the precursor **4** in 59% yield.

2.1.4. Optimization of protective groups for a boronic acid of BPA. Since the amide bond formation of BPA ethyl ester **13** and the precursor **4** did not proceed, we investigated suitable protective groups for a boronic acid of BPA (Fig. 2). A proper choice of protective groups of a boronic acid is important for the synthesis of biologically active boron compounds because the deprotection process is not an easy task at the end of the synthesis.[35,36] Although the deprotection reaction of the pinacol ester **14** did not proceed by the oxidative cleavage ($NaIO_4$, $AcONH_4$, acetone–H_2O), the fluoride ion (KHF_2), and the transesterification (phenylboronic acid, Et_2O–H_2O), pinanediol was found to be an effective protective group for BPA.[37–40] The pinanediol ester **15** underwent the transesterification with phenylboronic acid in Et_2O–H_2O to afford **13** in 34% yield and the yield increased up to 48% when the reaction was carried out in hexane–H_2O under pH ~ 3.[41]

2.1.5. Synthesis of BPA–Gd–DTPA complex. Synthesis of the BPA–Gd–DTPA complex is shown in Scheme 4. The amide formation reaction of the precursor **4** with the pinanediol-protected BPA **15** was carried out with 1,3-dicyclohexylcarbodiimide (DCC) in dichloromethane to give the desired product **16** in 84% yield. All ethyl ester groups of **16** were hydrolyzed with excess amounts of LiOH monohydrate and then the reaction mixture was acidified with 10% HCl (pH ~ 2) to give the corresponding hexacarboxylic acids **17** in 29% yield. Deprotection of the pinanediol group of **17** was carried out in the presence of an equivalent of phenylboronic acid in hexane–H_2O to afford the corresponding boronic acid **18** in 67% yield. The yield of **18** increased up to 89% when 2 equiv of phenylboronic acid were employed. Finally, the treatment of **18** with 1 equiv of gadolinium(III) chloride hexahydrate and sodium carbonate gave the desired BPA–Gd–DTPA complex **3** in 68% yield. The structure of **3** was confirmed by ESI-MS and elemental analysis.

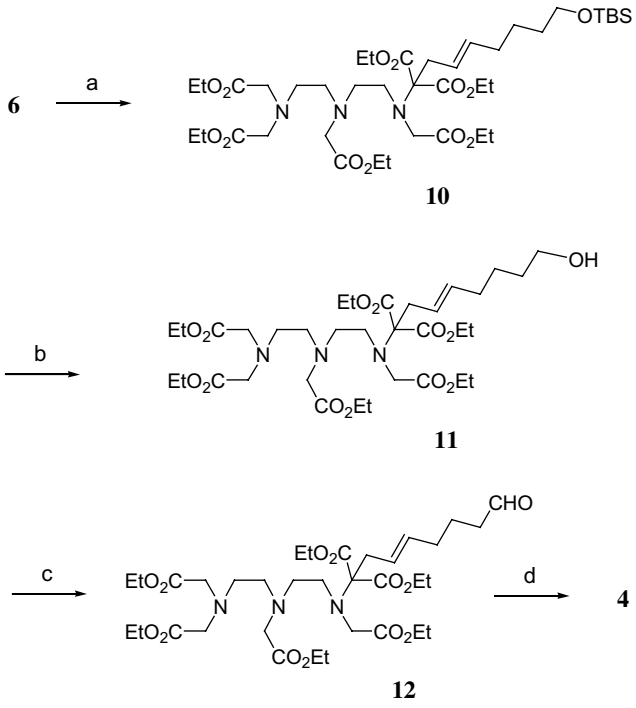

Scheme 3. Reagents and conditions: (a) **7**, $Pd(dba)_2$, dppe, THF, reflux; (b) TBAF, THF; (c) SO_3·pyridine, TEA, DMSO; (d) $NaClO_2$, NaH_2PO_4, 2-methyl-2-butene, THF–*t*-BuOH–H_2O.

2.2. Biodistribution study in vivo

2.2.1. Gadolinium concentrations in various tissues of tumor-bearing rats using prompt gamma-ray analysis (PGA). Biodistribution of gadolinium in vivo was examined using rats with a tumor implanted on their back. Compound **3** (0.048 M, 0.30 mL) was injected intravenously into a rat via the tail vein. At 20 and 60 min after injection, the rats were sacrificed by dislocation of the cervical vertebrae, and blood, liver, kidney, thigh muscle, brain, and tumor were excised. Gadolinium concentration in each tissue was determined by PGA. The results are shown in Figure 3a. The percentages of injected dose per 100 mg of tissue (%ID/100 mg tissue) are indicated in the vertical axes. The %ID values in the blood and the liver were 0.027 and 0.078, respectively, at 20 min after injection, and those values dropped to 0.0032 and 0.013, respectively, at 60 min. High accumulation was observed in the kidney and %ID values were 0.17 and 0.088 at 20 and 60 min after

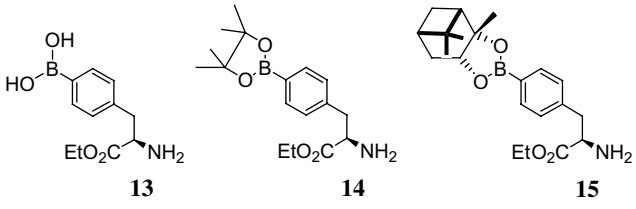

Figure 2.

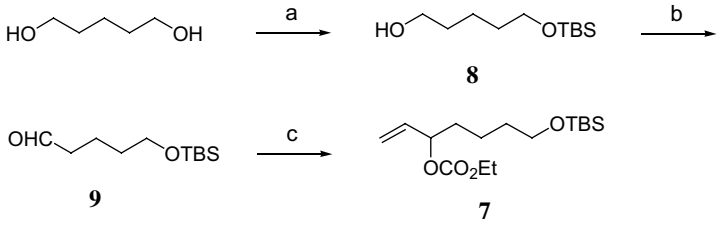

Scheme 2. Reagents and conditions: (a) i. TBSCl, imidazole, DMF, 0 °C; (b) TEMPO, NaClO, KBr, CH_2Cl_2–H_2O, 0 °C; (c) i. vinyl magnesium bromide, THF, −78 °C; ii. ethyl chloroformate.

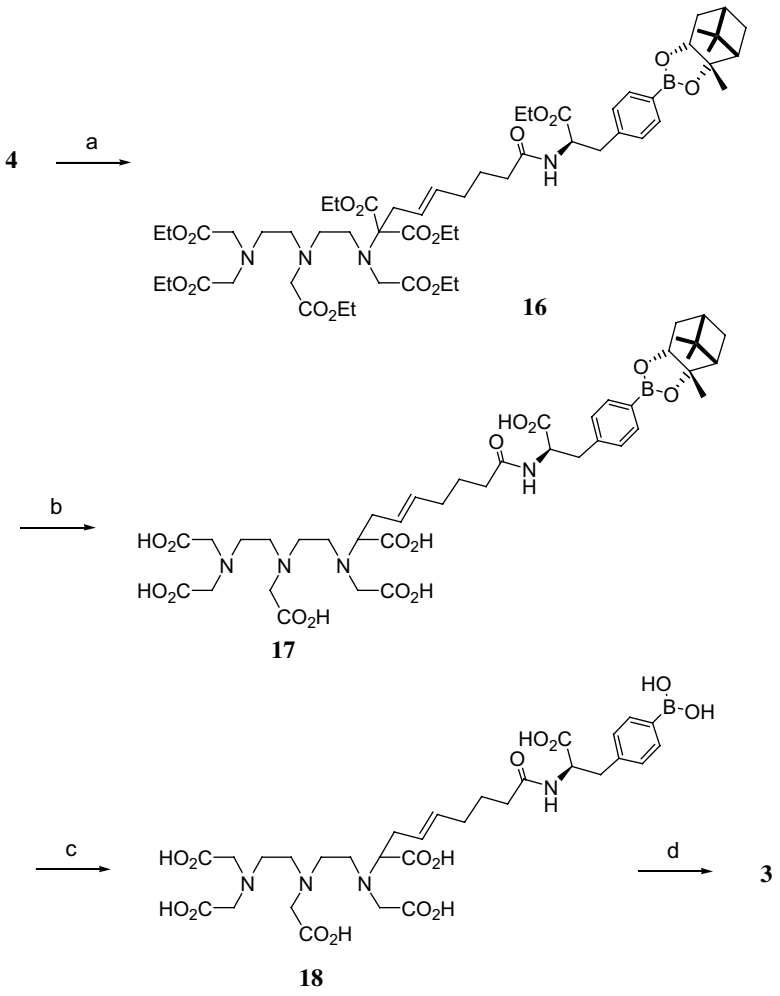

Scheme 4. Reagents and conditions: (a) **15**, DCC, CH_2Cl_2, 0 °C; (b) i. LiOH, H_2O; ii. 10% HCl (pH ~ 2); (c) phenylboronic acid (2 equiv) hexane–H_2O; (d) $GdCl_3 \cdot 6H_2O$, Na_2CO_3, MeOH–H_2O.

injection, respectively. Although gadolinium accumulation was very low in the muscle and the brain, the accumulation was observed in the tumor and the %ID values were 0.010 and 0.0025 at 20 and 60 min after injection, respectively. Figure 3b shows the biodistribution of the carborane–Gd–DTPA complex **2**, which was reported previously.[29,30] The gadolinium concentration of **2** in the blood was the same level as the BPA–Gd–DTPA **3**. The %ID values of **2** in the liver and the kidney were much lower than those of **3** and gadolinium accumulation was not observed in the brain and the tumor.

2.2.2. Boron distribution of tumor-bearing rats visualized by α-autoradiography (α-ARG). Compound **3** was dissolved in saline, and then the solution (0.048 M, 0.30 mL) was injected intravenously into a rat via the tail vein under the anesthesia by ether. At 20 and 60 min after the injection, the rats were sacrificed by an overdose of $CHCl_3$. The rats were coated completely with the carboxymethylcellulose (CMC–Na), and then frozen at −80 °C for an hour. After sectioning the frozen rats, the sections of 50 μm thick were obtained on adhesive tapes with Auto Cryotome at −20 °C, attached to the special tapes (CR-39, Baryotrack, 2 mm thick) for α-ARG, and then irradiated with thermal neutrons. Figure 4a and b show the cross section of the rat and the boron distribution visualized by α-ARG, respectively, at 20 min after injection of compound **3**. The parts visualized as white indicate the distribution of boron in Figure 4b. Since the tumor on the back of the rat was visualized, boron was accumulated significantly in the tumor. Furthermore, high accumulation of boron was observed in the intestines.

3. Discussion

The %ID values of **3** and **2** in the tumor at 20 min after injection were 0.0100 and 0.000878, respectively, and the tumor/blood ratios of those compounds were 0.380 and 0.0750, respectively. The tumor/blood ratio of **3** increased to 0.789 at 60 min, although the gadolinium concentration in the tumor was not detected at 60 min in the case of compound **2**. These results indicate that compound **3** possess higher tumor-selectivity than compound **2**. Compound **3** was highly accumulated into the liver and the kidney at 20 min after injection. However, the gadolinium concentrations of **3** in the liver and the kidney decreased at 60 min, and 16% and 53% of the gadolinium concentrations obtained at 20 min

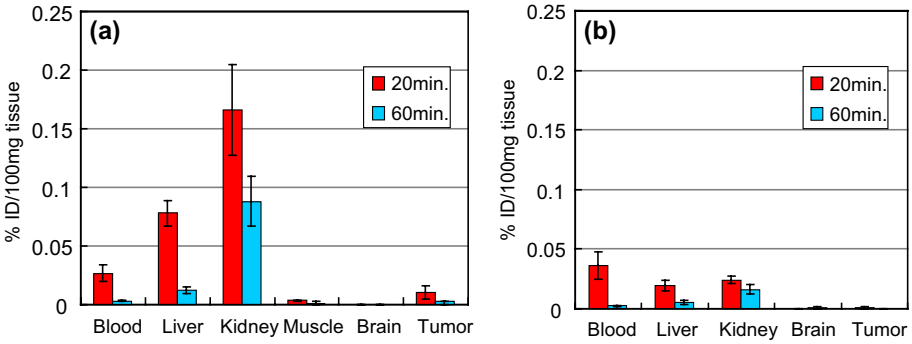

Figure 3. The distribution of Gd incorporated into various tissues of rats at 20 and 60 min after injection of BPA–Gd–DTPA **3** (a) and carborane–Gd–DTPA **2** (b).

were observed in the liver and the kidney, respectively. The gadolinium concentrations of **2** in the liver and the kidney at 60 min were 25% and 67% of those observed at 20 min. Therefore, it is considered that compound **3** would be metabolized and excreted more rapidly in comparison with compound **2**. These results correspond to the observation by α-autoradiography in Figure 4b. Perhaps, the compound **3** and its metabolite would be excreted directly in the bile via the liver or in the intestines. The tumor/muscle ratios of **3** were 2.73 at 20 min and 2.89 at 60 min, respectively, and no accumulation of **3** was observed in the brain.

4. Conclusion

We have succeeded in the synthesis of a new boron–gadolinium conjugated compound, BPA–Gd–DTPA complex (**3**), as an MRI contrast carrier for NCT. The higher accumulation of complex **3** was observed in the tumor tissue in comparison with the case of the carborane–Gd–DTPA complex **2** by the in vivo biodistribution experiments using PGA and α-autoradiography. In this regard, the BPA moiety is considered to play an important role for the accumulation of the Gd–DTPA complex in the tumor tissue. Since the various amino acids instead of BPA can be introduced into the DTPA framework through the amide bond formation, we believe that the current method described in this paper would be a very useful strategy not only for the synthesis of boron carriers on NCT but also for the development of biofunctional Gd–DTPA complexes.

5. Experimental

5.1. Chemistry

^{1}H NMR and ^{13}C NMR spectra were measured with JEOL JNM-GSX-270, JEOL JNM-AL-300, and JEOL JNM-AL-400 spectrometer. Chemical shifts of ^{1}H NMR and ^{13}C NMR were expressed in parts per million. IR spectra were measured with SHIMADZU FTIR-8200A. HPLC was performed with Mightysil RP-18 250-20 (5 μm) column. BPA (*L*/*D* = 72:28) was obtained from Hayashibara Biochemical Laboratories, Inc., Okayama, Japan. Most chemicals and solvents were analytical grade and used without further purification.

5.1.1. 5-(*tert*-Butyldimethylsilyloxy)pentanol 8. To a solution of imidazole (0.32 g, 4.6 mmol) in DMF (7.2 mL) at rt under Ar was added 1,5-pentanediol (2.1 mL, 20 mmol), and the mixture was stirred at 0 °C. To the mixture was added TBSCl (0.54 g, 3.6 mmol) at 0 °C, and the mixture was stirred for 15 min. The mixture was diluted with ether, and washed with water and brine. The organic layer was dried over anhydrous $MgSO_4$ and concentrated in vacuo. Purification by silica gel column chromatography (hexane/AcOEt = 4:1) gave **8** (0.55 g, 2.7 mmol, 74% yield): colorless oil; IR (neat) 3500–3000, 2931, 1255, 1101, 835 cm^{-1}; ^{1}H NMR (300 MHz, $CDCl_3$): δ 3.60 (t, J = 6.3 Hz, 2H), 3.57 (t, J = 6.3 Hz, 2H), 1.56–1.45 (m, 4H), 1.40–1.32 (m, 2H), 0.84 (s, 9H), 0.00 (s, 6H); ^{13}C NMR (400 MHz, $CDCl_3$): δ 62.9, 62.0, 32.3, 32.1, 25.8, 25.7, 21.8, 18.1, −5.4, −5.5. Anal. Calcd for $C_{11}H_{26}O_2Si$: C, 60.49; H, 12.00. Found: C, 60.33; H, 11.97.

5.1.2. 5-(*tert*-Butyldimethylsilyloxy)pentanal 9. To a solution of **8** (3.4 g, 15.6 mmol) in CH_2Cl_2 (63 mL) at 0 °C were added aqueous KBr (1.0 M, 1.56 mL, 1.56 mmol), 2,2,6,6-tetramethyl-1-piperidinyloxy, free radical (TEMPO) (0.049 g, 0.31 mmol), and a freshly prepared bleach solution (0.3 M, a 1:1 mixture of commercial bleach solution and saturated $NaHCO_3$, 62 mL, 18.7 mmol). After vigorous stirring for 2.5 h, the mixture was diluted with ether and washed with water and brine. The organic layer was dried over anhydrous $MgSO_4$, and concentrated in vacuo. Purification by silica gel column chromatography (hexane/AcOEt = 4:1) gave **9** (3.1 g, 14.3 mmol, 92% yield): colorless oil; IR (neat) 2952, 1749, 1255, 1101, 835 cm^{-1}; ^{1}H NMR (300 MHz, $CDCl_3$): δ 9.72 (t, J = 1.8 Hz, 1H), 3.58 (t, J = 6.3 Hz, 2H), 2.41 (dt, J = 6.7, 1.8 Hz, 2H), 1.70–1.60 (m, 2H), 1.54–1.45 (m, 2H), 0.84 (s, 9H), 0.00 (s, 6H); ^{13}C NMR (400 MHz, $CDCl_3$): δ 201.0, 62.0, 43.1, 31.7, 25.5, 18.2, 17.9, −5.7, −5.8. Anal. Calcd for $C_{11}H_{24}O_2Si$: C, 61.05; H, 11.18. Found: C, 60.94; H, 11.32.

5.1.3. The allylic carbonate 7. To a solution of **9** (2.7 g, 12.5 mmol) in THF (60 mL) at −78 °C under Ar was

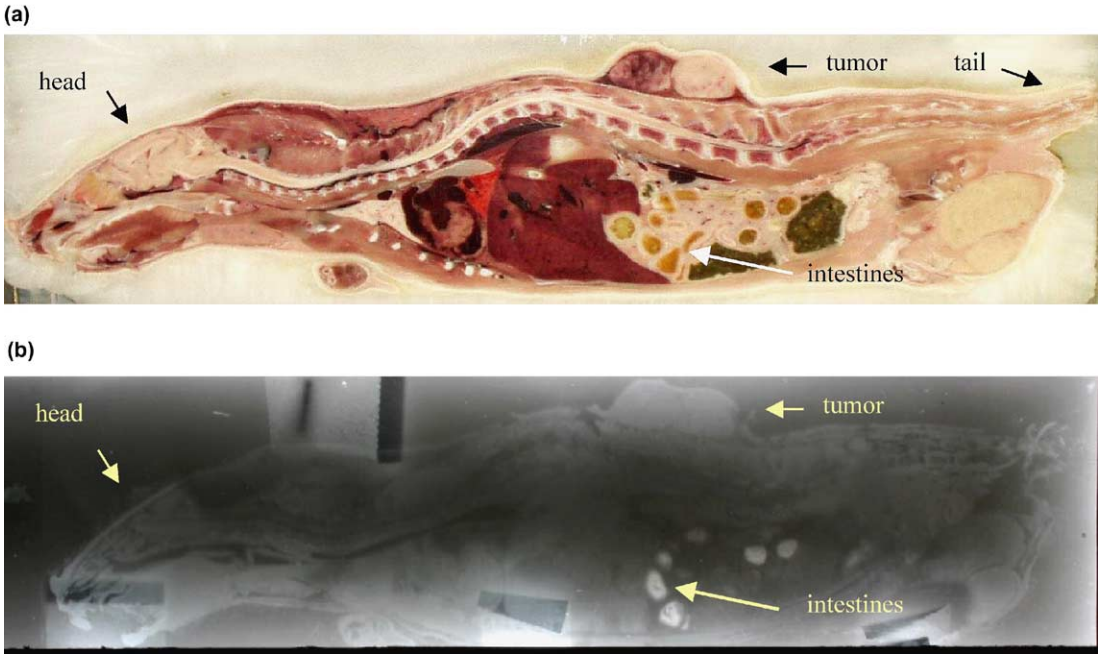

Figure 4. Cross section (a) and α-autoradiography (b) of a rat bearing AH109A tumor on the back at 20 min after injection of the compound **3**.

added vinyl magnesium bromide (1.0 M in THF solution, 15.0 mL, 15.0 mmol) over a period of 25 min. After being stirred for an hour at the same temperature, ethyl chloroformate (1.4 mL, 15.0 mmol) was added to the solution over a period of 10 min. After being stirred for an hour at rt, the mixture was quenched with saturated NH_4Cl at 0 °C, diluted with ether, and then washed with water and brine. The organic layer was dried over anhydrous $MgSO_4$ and concentrated in vacuo. Purification by silica gel column chromatography (hexane/AcOEt = 4:1) gave **7** (3.1 g, 9.8 mmol, 78% yield): yellow oil; IR (neat) 2952, 1747, 1647, 1257, 1101, 837, 775 cm^{-1}; ^1H NMR (300 MHz, $CDCl_3$): δ 5.75 (ddd, $J = 17.4$, 10.5, 6.9 Hz, 1H), 5.25 (d, $J = 17.4$ Hz, 1H), 5.16 (d, $J = 10.5$ Hz, 1H), 5.04–4.99 (m, 1H), 4.14 (q, $J = 6.9$ Hz, 2H), 3.56 (t, $J = 6.3$ Hz, 2H), 1.70–1.35 (m, 6H), 1.26 (t, $J = 6.9$ Hz, 3H), 0.84 (s, 9H), 0.00 (s, 6H); ^{13}C NMR (400 MHz, $CDCl_3$): δ 154.2, 135.8, 116.8, 78.3, 63.3, 62.4, 33.7, 25.7, 25.6, 21.1, 18.0, 14.0, −5.4, −5.5. Anal. Calcd for $C_{16}H_{32}O_4Si$: C, 60.72; H, 10.19. Found: C, 59.87; H, 9.88.

5.1.4. Allylation of the diethylenetriaminehexaacetic acid hexaethyl ester 6 with the allylic carbonate 7. A mixture of **6** (1.6 g, 2.6 mmol), **7** (1.3 g, 4.0 mmol), $Pd(dba)_2$ (0.30 g, 0.52 mmol), and dppe (0.31 g, 0.78 mmol) in THF (25 mL) was refluxed for two days under Ar. The mixture was cooled to rt, diluted with ether, and washed with water and brine. The organic layer was dried over anhydrous $MgSO_4$ and concentrated in vacuo. Purification by silica gel column chromatography (hexane/AcOEt = 1:1) gave **10** (1.9 g, 2.2 mmol, 83% yield): yellow oil; IR (neat) 2981, 1732, 1652, 1463, 1369, 1190, 1097, 1031 cm^{-1}; ^1H NMR (300 MHz, $CDCl_3$): δ 5.41 (br s, 2H), 4.17–4.05 (m, 12H), 3.54 (t, $J = 6.3$ Hz, 2H), 3.52 (s, 6H), 3.37 (s, 2H), 2.83–2.64 (m, 10H), 1.94 (m, 2H), 1.47–1.42 (m, 2H), 1.32–1.27 (m, 2H), 1.21 (t, $J = 7.2$ Hz, 18H), 0.84 (s, 9H), 0.00 (s, 6H); ^{13}C NMR (270 MHz, $CDCl_3$): δ 171.5, 171.2, 170.9, 169.3, 133.9, 123.9, 75.3, 62.9, 61.0, 60.3, 60.2, 60.1, 55.4, 55.3, 55.2, 53.9, 52.8, 52.4, 50.5, 37.9, 32.3, 25.9, 25.6, 18.3, 14.2, −5.2; MS (FAB), calcd for $C_{40}H_{74}SiN_3O_{13}$ (M+H) 832.4991, found: 832.5254. Anal. Calcd for $C_{40}H_{73}N_3O_{13}Si$: C, 57.74; H, 8.84; N, 5.05. Found: C, 57.60; H, 8.73; N, 4.92.

5.1.5. Desilylation of 10. To a solution of **10** (0.24 g, 0.29 mmol) in THF (1.5 mL) at rt was added TBAF (1.0 M in THF, 0.44 mL, 0.44 mmol), and the mixture was stirred for 10 h. The mixture was diluted with ether and washed with water and brine. The organic layer was dried over anhydrous $MgSO_4$ and concentrated in vacuo. Purification by silica gel column chromatography (hexane/AcOEt = 1:2) gave **11** (0.19 g, 0.26 mmol, 90% yield): yellow oil; IR (neat) 3550–3200, 2981, 1747, 1650, 1456, 1369, 1031 cm^{-1}; ^1H NMR (300 MHz, $CDCl_3$): δ 5.38 (br s, 2H), 4.13–4.01 (m, 12H), 3.52 (t, $J = 6.6$ Hz, 2H), 3.49 (s, 6H), 3.33 (s, 2H), 2.81–2.62 (m, 10H), 2.00 (br s, 1H), 1.93 (m, 2H), 1.50–1.42 (m, 2H), 1.36–1.29 (m, 2H), 1.18 (t, $J = 6.9$ Hz, 18H); ^{13}C NMR (300 MHz, $CDCl_3$): δ 171.2, 170.8, 170.5, 168.9, 133.2, 123.5, 74.6, 60.6, 59.9, 59.8, 59.6, 54.9, 54.8, 54.7, 53.3, 52.3, 51.7, 49.7, 37.3, 31.5, 24.9, 13.7; HRMS (ESI), calcd for $C_{34}H_{60}N_3O_{13}$ (M+H) 718.4121, found: 718.4121. Anal. Calcd for $C_{34}H_{59}N_3O_{13}$: C, 56.89, H, 8.28, N, 5.85. Found: C, 56.48, H, 8.38, N, 5.83.

5.1.6. The aldehyde 12. To a mixture of **11** (0.10 g, 0.14 mmol) and Et_3N (0.097 mL, 0.70 mmol) in DMSO (0.35 mL) at rt under Ar was added SO_3·pyridine complex (0.067 g, 0.42 mmol) in DMSO (0.35 mL), and the mixture was stirred for 30 min at rt. The mixture was

quenched with saturated NH_4Cl at 0 °C, diluted with ether, and then washed with water and brine. The organic layer was dried over anhydrous $MgSO_4$ and concentrated in vacuo. The pure compound **12** was obtained quantitatively (0.10 g, 0.14 mmol): yellow oil; IR (neat) 2981, 1747, 1446, 1369, 1031 cm^{-1}; ^1H NMR (300 MHz, $CDCl_3$): δ 9.73 (s, 1H), 5.42 (m, 2H), 4.19–4.06 (m, 12H), 3.53 (s, 6H), 3.38 (s, 2H), 2.83–2.73 (m, 8H), 2.67 (d, J = 5.1 Hz, 2H), 2.40 (t, J = 6.6 Hz, 2H), 2.00 (m, 2H), 1.66–1.61 (m, 2H), 1.23 (t, J = 7.2 Hz, 18H); ^{13}C NMR (270 MHz, $CDCl_3$): δ 202.3, 171.5, 171.3, 171.0, 169.3, 132.6, 125.2, 75.2, 61.1, 60.3, 60.2, 60.1, 55.4, 55.3, 55.2, 53.9, 52.8, 52.4, 50.4, 43.0, 37.8, 31.7, 21.5, 14.2; HRMS (ESI), calcd for $C_{34}H_{57}N_3O_{13}$-Na (M+Na) 738.3734, found: 738.3734.

5.1.7. Synthesis of the precursor 4. To a solution of **12** (3.0 g, 4.2 mmol) in *t*-BuOH (21 mL) and water (21 mL) at rt were added 2-methyl-2-butene (2.7 mL, 25 mmol), NaH_2PO_4 (1.5 g, 13 mmol), and $NaClO_2$ (1.1 g, 13 mmol), and the mixture was stirred vigorously for 11 h at rt. The mixture was diluted with AcOEt and washed with water and brine. The organic layer was dried over anhydrous Na_2SO_4 and concentrated in vacuo. Purification by silica gel column chromatography (hexane/AcOEt = 1:10) gave **4** (1.8 g, 2.5 mmol, 59% yield): yellow oil; IR (neat) 3200–2800, 1749, 1652, 1456, 1028 cm^{-1}; ^1H NMR (400 MHz, $CDCl_3$): δ 5.42 (br s, 2H), 4.19–4.08 (m, 12H), 3.57 (s, 2H), 3.55 (s, 4H), 3.42 (s, 2H), 2.90–2.72 (m, 10H), 2.34 (t, J = 7.2 Hz, 2H), 2.04 (m, 2H), 1.68 (quint, J = 8.0 Hz, 2H), 1.26–1.22 (m, 18H); ^{13}C NMR (400 MHz, $CDCl_3$): δ 177.3, 171.4, 170.8, 170.7, 169.1, 132.6, 124.7, 74.8, 60.8, 60.0, 59.9, 59.9, 54.7, 53.3, 52.3, 52.2, 51.6, 49.7, 37.4, 32.9, 31.4, 23.9, 13.8; HRMS (ESI), calcd for $C_{34}H_{57}N_3O_{14}Na$ (M+Na) 754.3733, found: 754.3732. Anal. Calcd for $C_{34}H_{57}N_3O_{14}\cdot H_2O$: C, 54.46; H, 7.93; N, 5.60. Found: C, 54.08; H, 7.63; N, 5.90.

5.1.8. BPA ethyl ester 13. A solution of thionyl chloride (0.13 mL, 1.8 mmol) in EtOH (1.5 mL) was stirred for an hour at 0 °C under Ar. To the mixture was added BPA (*L*/*D* = 72:28, 0.11 g, 0.50 mmol), and the solution was stirred for 5 min at 0 °C and then stirred for two days at rt. The reaction was neutralized with saturated $NaHCO_3$ at 0 °C, and the mixture was diluted with AcOEt and washed with water and brine. The organic layer was dried over anhydrous Na_2SO_4 and concentrated in vacuo. Purification by recrystallization (CH_3Cl/ether) gave **13** (96 mg, 0.40 mmol, 81% yield): white solid; IR (KBr) 3380, 2981, 1732, 1614, 1249 cm^{-1}; ^1H NMR (400 MHz, $CDCl_3$): δ 7.84 (d, J = 7.5 Hz, 2H), 7.14 (d, J = 7.5 Hz, 2H), 4.16–4.01 (m, 2H), 3.81 (dd, J = 9.2, 4.4 Hz, 1H), 3.16 (dd, J = 13.6, 4.4 Hz, 1H), 2.76 (dd, J = 13.2, 9.6 Hz, 1H), 2.34 (br s, 1H), 1.22 (t, J = 7.2 Hz, 3H); ^{13}C NMR (400 MHz, $CDCl_3$): δ 173.5, 137.3, 134.0, 128.2, 61.3, 58.1, 39.9, 13.8; HRMS (ESI), calcd for $C_{13}H_{21}BNO_4$ (M+C_2H_4+H) 266.1558, found: 266.1558.

5.1.9. Protection of BPA ethyl ester by pinanediol. To a solution of **13** (0.28 g, 1.2 mmol) in CH_2Cl_2 (2 mL) at rt was added (1*S*,2*S*,3*R*,5*S*)-(+)-pinanediol (0.20 g, 1.2 mL) in CH_2Cl_2 (0.5 mL), and the mixture was stirred for 2.5 h at rt. The mixture was filtrated, concentrated, and then purified by preparative thin layer chromatography with AcOEt to give **15** (0.45 g, 1.2 mmol, >99% yield): yellow oil; IR (neat) 3384, 2933, 1735, 1612, 1236 cm^{-1}; ^1H NMR (400 MHz, $CDCl_3$): δ 7.74 (d, J = 8.0 Hz, 2H), 7.20 (d, J = 8.0 Hz, 2H), 4.43 (dd, J = 9.0, 1.6 Hz, 1H), 4.15 (q, J = 7.0 Hz, 2H), 3.70 (dd, J = 8.0, 5.2 Hz, 1H), 3.09 (dd, J = 13.2, 5.2 Hz, 1H), 2.85 (dd, J = 13.2, 8.0 Hz, 1H), 2.43–2.37 (m, 1H), 2.22–2.20 (m, 1H), 2.13 (t, J = 6.0 Hz, 1H), 1.96–1.91 (m, 2H), 1.46 (s, 3H), 1.30 (s, 3H), 1.23 (t, J = 7.0 Hz, 3H), 1.19 (s, 1H), 0.87 (s, 3H); ^{13}C NMR (400 MHz, $CDCl_3$): δ 173.9, 139.9, 134.3, 128.0, 85.3, 77.4, 60.0, 55.1, 50.7, 40.7, 38.9, 37.5, 34.9, 28.1, 26.5, 25.9, 23.4, 13.7; HRMS (ESI), calcd for $C_{21}H_{30}BNO_4$ (M+H) 372.2340, found: 372.2340.

5.1.10. DCC coupling of 4 with 15. To a solution of **4** (1.6 g, 2.2 mmol) and **15** (0.81 g, 2.2 mmol) in CH_2Cl_2 (7 mL) at 0 °C under Ar was added DCC (0.45 g, 2.2 mmol) dissolved in CH_2Cl_2 (7 mL). The mixture was stirred for 2 h at 0 °C and then stirred for 5 h at rt. The solution was filtrated, and the filtrate was diluted with AcOEt and washed with water and brine. The organic layer was dried over anhydrous Na_2SO_4 and concentrated in vacuo. Purification by silica gel column chromatography (hexane/AcOEt = 1:2) gave **16** (0.30 g, 0.28 mmol, 84% yield): yellow oil; IR (neat) 3375, 2979, 1749, 1616, 1471, 1224 cm^{-1}; ^1H NMR (400 MHz, $CDCl_3$): δ 7.70 (d, J = 8.0 Hz, 2H), 7.14 (d, J = 8.0 Hz, 2H), 6.30 (d, J = 7.6 Hz, 1H), 5.49–5.34 (m, 2H), 4.81 (q, J = 7.6 Hz, 1H), 4.42 (d, J = 8.4 Hz, 1H), 4.16–4.06 (m, 14H), 3.55 (s, 2H), 3.53 (s, 4H), 3.38 (s, 2H), 3.17–3.06 (m, 2H), 2.86–2.67 (m, 10H), 2.42–2.34 (m, 1H), 2.21–2.10 (m, 4H), 1.91–1.94 (m, 4H), 1.65–1.57 (m, 2H), 1.44 (s, 3H), 1.26 (s, 3H), 1.23–1.17 (m, 22H), 0.87 (s, 3H); ^{13}C NMR (400 MHz, $CDCl_3$): δ 172.5, 171.5, 171.4, 171.3, 171.1, 170.8, 169.3, 139.4, 134.6, 132.7, 128.42, 124.9, 85.8, 77.8, 74.9, 60.9, 60.0, 59.8, 55.1, 54.9, 53.4, 53.2, 52.9, 52.7, 52.5, 52.0, 51.1, 49.9, 39.2, 37.8, 37.6, 37.4, 35.2, 34.3, 31.0, 28.4, 26.7, 26.1, 24.2, 23.7, 13.9; HRMS (ESI), calcd for $C_{55}H_{85}BN_4O_{17}Na$ (M+Na) 1107.5895, found: 1107.5905. Anal. Calcd for $C_{55}H_{85}BN_4O_{17}$: C, 60.88; H, 7.90; N, 5.16. Found: C, 60.52; H, 7.94; N, 5.50.

5.1.11. Deprotection of the ethyl esters 16. To a solution of **16** (83 mg, 0.077 mmol) in EtOH (4 mL) was added $LiOH\cdot H_2O$ (52 mg, 1.2 mmol) dissolved in water (1 mL), and the mixture was stirred for two days at rt. The mixture was concentrated, diluted with a little amount of water, and then washed with ether. To the water layer was added aq 10% HCl until a white solid was precipitated. The white solid was washed with water and then dried in vacuo to give **17** (19 mg, 0.022 mmol, 29% yield): white solid; IR (KBr) 3300–2700, 1732, 1650, 1398, 1234 cm^{-1}; ^1H NMR (400 MHz, CD_3OD): δ 7.62 (d, J = 8.0 Hz, 2H), 7.20 (d, J = 8.0 Hz, 2H), 5.40 (br s, 2H), 4.65–4.64 (m, 2H), 4.43 (d, J = 8.0 Hz, 1H), 4.00 (br s, 2H), 3.67–3.12 (m, 16H), 2.93 (dd, J = 13.8, 4.4 Hz, 1H), 2.43–2.37 (m, 3H), 2.19–2.05 (m, 4H), 1.89–1.87 (m, 4H), 1.51 (br s, 2H), 1.42 (s, 3H),

1.28 (s, 3H), 1.11 (d, $J = 10.8$ Hz, 1H), 0.87 (s, 3H); ^{13}C NMR (400 MHz, CD_3OD): δ 176.1, 175.9, 175.3, 174.8, 174.7, 174.4, 170.2, 141.9, 135.8, 134.1, 129.7, 127.7, 87.4, 79.4, 66.4, 56.0, 55.7, 54.7, 54.2, 53.9, 52.9, 52.7, 50.8, 50.7, 40.8, 39.2, 38.5, 36.5, 36.0, 34.7, 34.4, 32.7, 29.1, 27.5, 27.3, 26.2, 24.3; MS (ESI), calcd for $C_{40}H_{57}BN_4O_{15}$ (M^+) 844.3921, found: 844.6067; HPLC analysis: retention time, 34.9 min (ODS, MeOH/H_2O = 5:2, 4.5 mL/min). Anal. Calcd for $C_{40}H_{57}BN_4O_{15}\cdot H_2O$: C, 55.69; H, 6.89; N, 6.49. Found: C, 55.69; H, 6.94; N, 6.37.

5.1.12. Deprotection of the pinanediol ester 17. A mixture of **17** (0.23 g, 0.27 mmol) and phenylboronic acid (65 mg, 0.54 mmol) in hexane (100 mL), MeOH (35 mL), and water (70 mL) was vigorously stirred at rt. After 30 min, the hexane layer was removed and hexane (100 mL) was added to the aqueous solution. After 30 min of stirring, the hexane layer was removed again. This procedure was repeated several times until the pinanediol protective group of **17** was transferred to phenylboronic acid. After the deprotection proceeded completely, the aqueous layer was washed with ether in order to remove excess phenylboronic acid. The mixture was concentrated in vacuo to give **18** (0.17 g, 0.24 mmol, 89% yield): white solid; IR (KBr) 3350–2650, 1770, 1652, 1398, 1226, 1037 cm^{-1}; ^1H NMR (400 MHz, CD_3OD): δ 7.61 (br s, 2H), 7.21 (d, $J = 7.6$ Hz, 2H), 5.43 (br s, 2H), 4.68 (br s, 1H), 4.00 (br s, 2H), 3.61–3.20 (m, 16H), 2.97 (d, $J = 13.7$, 4.2 Hz, 1H), 2.53–2.37 (m, 2H), 2.15 (br s, 2H), 1.90 (br s, 2H), 1.55 (br s, 2H); ^{13}C NMR (400 MHz, CD_3OD): δ 176.0, 175.3, 175.0, 174.4, 170.5, 140.6, 135.0, 134.1, 129.5, 127.7, 66.6, 56.2, 55.9, 54.8, 54.1, 53.8, 53.1, 50.9, 38.4, 36.0, 34.2, 32.7, 26.3; HPLC analysis: retention time, 22.0 min (ODS, MeOH/H_2O = 1:2, 4.5 mL/min). Anal. Calcd for $C_{30}H_{43}BN_4O_{15}\cdot C_2H_4$: C, 52.04; H, 6.41; N, 7.59. Found: C, 55.08; H, 6.39; N, 7.46.

5.1.13. BPA–Gd–DTPA complex 3. To a solution of **18** (58 mg, 0.082 mmol) in MeOH (4.0 mL) and water (1.0 mL) at rt was added $GdCl_3\cdot 6H_2O$ (30 mg, 0.082 mmol) in water (1.0 mL), and the mixture was stirred for 10 h at rt. The mixture was neutralized with aqueous Na_2CO_3 (0.24 M) and then stirred for an hour. The solution was concentrated and the residue was purified by HPLC (ODS, MeOH/H_2O = 1:2, retention time; 12 min, 4.5 mL/min) to give **3** (53 mg, 0.056 mmol, 68% yield): white solid; IR (KBr) 3674–3000, 2977, 1652, 1398, 1272, 1095 cm^{-1}; HPLC analysis: retention time, 12.3 min (ODS, MeOH/H_2O = 1:2, 4.5 mL/min); MS (ESI), calcd for $C_{32}H_{41}BGdN_4Na_3O_{15}$ (MH^+) 960.1688, found: 959.7672. Anal. Calcd for $C_{30}H_{37}BGdN_4Na_3O_{15}\cdot 6H_2O$: C, 34.69; H, 4.75; N, 5.39. Found: C, 35.24; H, 4.45; N, 5.30.

5.2. In vivo biodistribution

5.2.1. Biodistribution of gadolinium using prompt gamma-ray analysis (PGA). The tumors (AH109A-ascitic hepatoma) were implanted into the thighs of the six Donryu Rats weighing 190–200 g. Eight days after transplantation, the tumors grew up to an average weight of 2.7 g. A solution of the compound **3** in saline (3 mL, 0.048 M) was injected intravenously into a rat via the tail vein under the anesthesia by ether. At 20 and 60 min after the injection, the rats were sacrificed by a dislocation of the cervical vertebrae, and blood, liver, kidney, thigh muscle, brain, and tumor were excised. Gadolinium concentrations in those organs were measured with PGA.

5.2.2. Biodistribution of boron using α-autoradiography (α-ARG). A solution of the compound **3** in saline (3 mL, 0.048 M) was injected intravenously into a rat via the tail vein under the anesthesia by ether. At 20 min after the injection, the rat was sacrificed by an overdose of $CHCl_3$. The rat was coated completely with the sodium salt of 3.5% carboxymethylcellulose (CMC–Na) and then frozen at −80 °C for an hour. After sectioning the frozen rats, the sections of 50 μm thick were obtained on adhesive tapes with Auto Cryotome at −20 °C and then dried enough in the Cryotome at −20 °C for a few days. The sections were attached to the special tapes (CR-39, Baryotrack, 2 mm thick) for α-ARG. After irradiation with thermal neutrons (1.7×10^{13} n/cm^2), the sections on the Baryotrack were etched with 5 N NaOH aqueous solution for 3 h at 60 °C, and then boron distribution was visualized by the irradiation of a fluorescent light.

Acknowledgements

We thank Dr. M. Kawate (Neutron Science Laboratory, Institute for Solid State Physics, The University of Tokyo) for experimental supports of the prompt gamma-ray analysis.

References and notes

1. Sloway, A. H.; Tjarks, W.; Barnum, B. A.; Rong, F.-G.; Barth, R. F.; Wyzlic, I. M.; Wilson, J. G. *Chem. Rev.* **1998**, *98*, 1515–1562.
2. Barth, R. F.; Soloway, A. H.; Goodman, J. H.; Gahbauer, R. A.; Gupta, N.; Blue, T. E.; Yang, W.; Tjarks, W. *Neurosurgery* **1999**, *44*, 433–450.
3. Coderre, J. A.; Morris, G. M. *Radiat. Res.* **1999**, *151*, 1–18.
4. Godwin, J. T.; Farr, L. E.; Sweet, W. H.; Robertsson, J. S. *Cancer* **1955**, *8*, 601–615.
5. Snyder, H. R.; Reedy, A. J.; Lennarj, W. J. *J. Am. Chem. Soc.* **1958**, *80*, 835–838.
6. Ichihashi, M.; Nakanishi, T.; Mishima, Y. *J. Invest. Dermatol.* **1982**, *78*, 215–218.
7. Kulvik, M.; Vähätalo, J.; Buchar, E.; Färkkilä, M.; Järviluoma, E.; Jääskeläinen, J.; Kr'iz', O.; Laakso, J.; Rasilainen, M.; Ruokonen, I.; Kallio, M. *Eur. J. Pharm. Sci.* **2003**, *18*, 155–163.
8. Soloway, A. H.; Hatanaka, H.; Davis, M. A. *J. Med. Chem.* **1967**, *10*, 714–717.
9. Hatanaka, H.; Sano, K.; Yasukochi, H. In *Progress in Neutron Capture Therapy for Cancer*; Allen, B. J., Moore, D. E., Harrington, B. V., Eds.; Plenum: New York, 1992; pp 561–568.
10. Hatanaka, H.; Nakagawa, Y. *Int. J. Radiat. Oncol. Bio. Phys.* **1994**, *28*, 1061–1066.
11. Hatanaka, H.; Nakagawa, Y. *J. Neuro-Oncol.* **1997**, *33*, 105–115.

12. Takahashi, Y.; Imahori, Y.; Mineura, K. *Clin. Cancer Res.* **2003**, *9*, 5888–5895.
13. Kabalka, G. W.; Davis, M.; Bendel, P. *Magn. Reson. Med.* **1988**, *8*, 231–237.
14. Kabalka, G. W.; Tang, C.; Bendel, P. *Neuro-Oncology* **1997**, *33*, 153–161.
15. Bendel, P.; Zilberstein, J.; Salomon, Y. *Magn. Reson. Med.* **1994**, *32*, 170–174.
16. Bradshaw, K. M.; Schweizer, M. P.; Glover, G. H.; Hadley, J. R.; Tippetts, R.; Tang, P.-P.; Davis, W. L.; Heilbrum, M. P.; Johnson, S.; Ghanem, T. *Magn. Reson. Med.* **1995**, *34*, 48–56.
17. Straubinger, R. M.; Kahl, S. B.; Koo, M. S.; Alletto, J. J.; Mazurchuk, R.; Chau, R. I.; Thamer, S. L.; Fiel, R. J. *J. Magn. Reson. Im.* **1993**, *3*, 351–356.
18. Combs, M. J.; Mulder, R. U.; Berr, S. S.; Oveissi, C.; Kahl, S. B. In *Cancer Neutron Capture Therapy*; Mishima, Y., Ed.; Plenum: New York, 1996; pp 239–244.
19. Weinmann, H. J.; Brasch, R. C.; Press, W. R.; Wesbey, G. E. *AJR* **1984**, *142*, 619–624.
20. Gries, H.; Miklautz, H. *Physiol. Chem. Phys. Med. NMR* **1984**, *19*, 105–112.
21. Caravan, P.; Ellison, J. J.; McMurry, T. J.; Lauffer, R. B. *Chem. Rev.* **1999**, *99*, 2293–2352.
22. Tóth, É.; Burai, L.; Merbach, A. E. *Coord. Chem. Rev.* **2001**, *216–217*, 363–382.
23. Stack, J. P.; Antoun, N. M.; Jenkins, J. P. R.; Metcalfe, R.; Isherwood, I. *Neuroradiology* **1988**, *30*, 145–154.
24. Runge, V. M.; Jacobson, S.; Wood, M. L.; Kaufman, D.; Adelman, L. S. *Radiology* **1988**, *166*, 835–838.
25. Shibata, Y.; Matsumura, A.; Yamamoto, T.; Nakagawa, K.; Yoshii, Y.; Nose, T.; Sakata, I.; Nakajima, S.; Hayakawa, Y.; Ono, K. *J. Exp. Clin. Cancer Res.* **1998**, *17*, 285–289.
26. Matsumura, A.; Shibata, Y.; Nakagawa, K.; Yamamoto, T.; Yoshizawa, T.; Yoshii, Y.; Nose, T.; Sakata, I.; Nakajima, S.; Miwa, N. In *Cancer Neutron Capture Therapy*; Mishima, Y., Ed.; Plenum: New York, 1996; pp 245–250.
27. Matsumura, A.; Shibata, Y.; Yamamoto, T.; Nakagawa, K.; Yasuda, S.; Nakajima, S.; Sakata, I.; Yoshizawa, T.; Nose, T. *Neurol. Med.-Chir.* **1997**, *37*, 327–331.
28. Nemoto, H.; Cai, J.; Nakamura, H.; Fujiwara, M.; Yamamoto, Y. *J. Organomet. Chem.* **1999**, *581*, 170–175.
29. Girald, F.; Nakamura, H.; Fukuda, H.; Yamamoto, Y.; Yoahida, K. In *Recent Advances in Biomedical Imaging*; Ishii, Y., et al., Eds.; Elsevier Science: Amsterdam, 1997; pp 201–207.
30. Nakamura, H.; Fukuda, H.; Girald, F.; Kobayashi, T.; Hiratsuka, J.; Akaizawa, T.; Nemoto, H.; Cai, J.; Yoshida, K.; Yamamoto, Y. *Chem. Pharm. Bull.* **2000**, *48*, 1034–1038.
31. Yamamoto, Y. *Pure Appl. Chem.* **2003**, *75*, 1343–1348.
32. Sieving, P. F.; Watson, A. D.; Rocklage, S. M. *Bioconjugate Chem.* **1990**, *1*, 65.
33. Gries, H.; Miklautz, H. *Physiol. Chem. Phys. Med. NMR* **1984**, *16*, 105.
34. Tsuji, J.; Shimizu, I.; Mikami, I.; Ohashi, Y.; Sugiura, T.; Takahashi, K. *J. Org. Chem.* **1985**, *50*, 1523–1529.
35. Nakamura, H.; Fujiwara, M.; Yamamoto, Y. *J. Org. Chem.* **1998**, *63*, 7529–7530.
36. Nakamura, H.; Fujiwara, M.; Yamamoto, Y. *Bull. Chem. Soc. Jpn.* **2000**, *73*, 231–235.
37. Matteson, D. S.; Kim, G. Y. *Org. Lett.* **2002**, *4*, 2153–2155.
38. Matteson, D. S.; Lu, J. *Tetrahedron: Asymmetry* **1998**, *9*, 2423–2436.
39. Decicco, C. P.; Song, Y.; Evans, D. A. *Org. Lett.* **2001**, *3*, 1029–1032.
40. Coutts, S. J.; Adams, J.; Krolikowski, D.; Snow, R. J. *Tetrahedron Lett.* **1994**, *35*, 5109–5112.
41. Asano, T.; Nakamura, H.; Uehara, Y.; Yamamoto, Y. *ChemBioChem* **2004**, *5*, 483–490.